

Nonmonotonic superconducting transitions in mesoscopic Al structures induced by radio-frequency radiation

C. Strunk, V. Bruyndoncx, C. Van Haesendonck, V. V. Moshchalkov, and Y. Bruynseraede

Laboratorium voor Vaste-Stoffysika en Magnetisme, Katholieke Universiteit Leuven, Celestijnenlaan 200 D, B-3001 Leuven, Belgium

B. Burk, C.-J. Chien, and V. Chandrasekhar

Department of Physics and Astronomy, Northwestern University, 2145 Sheridan Road, Evanston, Illinois 60208

(Received 8 February 1996)

The recently reported and hitherto poorly understood resistance anomalies at the superconducting transition of quasi-one-dimensional mesoscopic Al structures can be induced by radio-frequency radiation. We show that these anomalies are correlated with changes in the voltage-current characteristics which are created in the presence of the radiation *below* the superconducting transition. The anomalies appear to be closely related to the creation of localized phase-slip centers by the radio-frequency radiation. [S0163-1829(96)04518-3]

Superconductivity in mesoscopic systems has received considerable experimental and theoretical interest in recent years.¹ An intriguing new phenomenon has been observed in superconducting (SC) mesoscopic Al lines² and loops^{3,4} when the dimensions of these samples are comparable to or smaller than the SC coherence length $\xi(T)$. A pronounced resistance overshoot is observed in the $R(T)$ curves just before reaching the normal-state resistance R_N . Although several explanations have been proposed^{2,4,5} to understand the enhancement of the resistance above its normal-state value, its exact origin is still unknown. The anomaly is believed to be related to the quasi-one-dimensional (quasi-1D) line structure and to the fact that the distance between the measuring probes becomes comparable to the characteristic length scales governing the SC transition.

It is well known that in SC lines having a width below $\xi(T)$ the onset of the resistive behavior is caused by the local, thermally activated creation of phase-slip centers (PSC's).⁶ Around the induced localized resistive spots an area of non-equilibrium superconductivity is created^{7,8} which is characterized by the difference between quasiparticle and Cooper pair electrochemical potentials μ_{QP} and μ_{CP} . Equilibrium is restored only on a length scale $\lambda_{Q^*}(T)$ which is considerably larger than $\xi(T)$. More recently, Kwong *et al.*⁹ have shown that a resistance overshoot can be created in the vicinity of a normal/superconducting (N/S) interface, supporting the importance of charge imbalance for the effect.

In this paper, we present experimental evidence that the resistance anomaly occurs in the superconducting state and can be controlled in *homogeneous* mesoscopic Al samples by applying radio-frequency (rf) radiation. We believe that the anomaly can be explained as a charge imbalance phenomenon arising from the local creation of PSC's by rf irradiation, and is directly related to changes in the voltage-current $V(I)$ characteristics induced by the radiation.

Samples were prepared by thermal evaporation of 99.999% pure Al onto oxidized Si wafers, previously patterned by standard *e*-beam lithography techniques. Scanning electron and atomic force microscopy revealed a smooth Al surface with no major cracks or holes appearing down to the nanometer scale. The sheet resistance of the 43 nm thick

Al films was 0.6Ω , giving an elastic mean free path $l \cong 16$ nm.¹⁰ For this l value we estimated the relevant characteristic lengths as $\xi(T) = 0.85[\xi_0 l / (1 - T/T_c)]^{1/2} \cong 0.13(1 - T/T_c)^{-1/2} \mu\text{m}$ and $\lambda_{Q^*}(T) = [D\tau_{Q^*}(T)]^{1/2} \cong 3.4(1 - T/T_c)^{-1/4} \mu\text{m}$. D is the electronic diffusion constant and $\tau_{Q^*}(T) = [4k_B T_c \tau_{in}] / [\pi \Delta(T)]$.^{11,12} $\Delta(T)$ is the energy gap and the inelastic scattering time τ_{in} , which depends on the degree of disorder, was estimated to be about 4 ns.¹¹

Figure 1 shows a schematic of a typical device. It consists of $0.13 \mu\text{m}$ wide lines, interrupted by a square loop with $1 \mu\text{m}$ outer diameter. Two pairs of voltage leads are attached on both sides of the loop. The distance between the voltage probes and the loop was 2 and $3 \mu\text{m}$, respectively. For smaller distances, the basic results remain unchanged. The linewidth of the current and voltage leads is kept constant at $0.13 \mu\text{m}$ to a distance of $7 \mu\text{m}$ from the sample in order to minimize the influence of the wide parts of the contacts on the measurement. We will focus here on the properties of the samples in zero magnetic field; the pronounced influence of a perpendicular magnetic field will be analyzed in a subsequent paper.

The transport measurements have been performed with a PAR 124 A lock-in amplifier for ac measurements at 27 Hz and a HP 34420 nanovoltmeter for dc measurements of the $V(I)$ characteristic. All leads (except for the coaxial cable

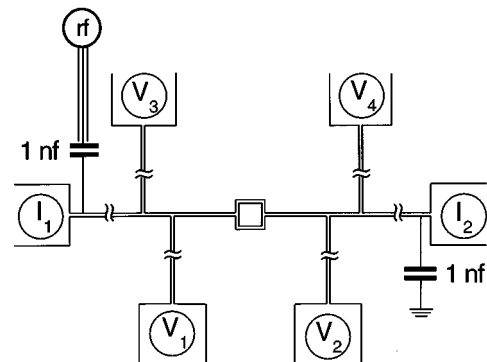


FIG. 1. Typical six-terminal layout with the rf current passed through the current contacts I_1 and I_2 .

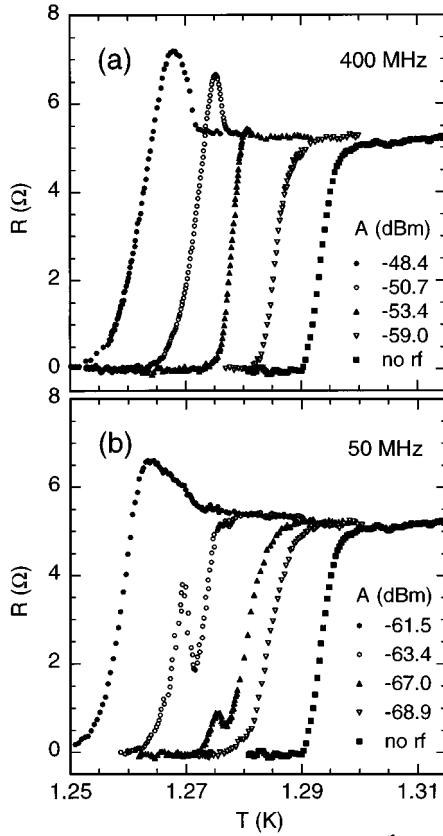


FIG. 2. $R(T)$ curves measured over segment V_1/V_3 for an applied rf signal of different amplitudes and of frequency (a) 400 MHz and (b) 50 MHz.

which is used to bring down the rf signal) are shielded by π filters with a cutoff frequency of 1 MHz. The six sample leads consist of stainless steel coaxial cables, providing a further damping for rf interference with frequencies above 1 GHz. The rf signal, generated by a Rhode and Schwarz SMY-02 source, is transmitted by a coaxial cable in a separate tube and coupled with small capacitors to the current leads of the sample (Fig. 1). Due to the changing impedance of the sample as it goes through the superconducting transition, it is difficult to determine the actual amount of rf power applied to the sample for different frequencies. Nevertheless, a comparative study of the response of different segments of the same sample at fixed frequency is possible, since the rf signal is applied simultaneously to all segments of the sample and the wavelength of the radiation is large in comparison to the sample dimensions.

Figure 2(a) shows the superconducting transition for the line segment between voltage leads V_1 and V_3 (see Fig. 1) for various amplitudes of an applied rf field of 400 MHz. The trace for -48.8 and -50.7 dB power is similar to the resistance anomaly that has been observed previously²⁻⁴ with no intentionally applied rf field. With proper shielding, the resistance anomaly disappears, as can be seen in the trace of Fig. 2(a) with no applied rf radiation. Introduction of a small amount of rf first leads to a decrease in T_c , which may be due to pair breaking or joule heating of the sample. For higher rf power, pronounced resistance maxima can be induced, with R exceeding R_N by up to 30%. Similar trends are observed up to our maximum irradiation frequency of 2

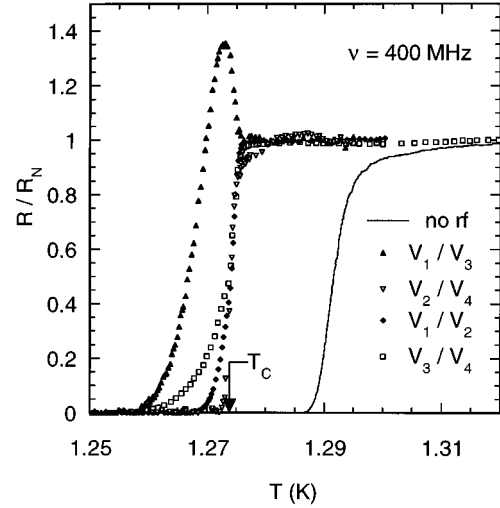


FIG. 3. Normalized $R(T)$ curves for an applied rf disturbance of 400 MHz and -50 dB power measured across different segments of the sample. A clear bump shows up across segment V_1/V_3 only. Note that the depression of T_c is the same for all segments and the resistance bump in segment V_1/V_3 arises indeed below T_c . For comparison, the solid line shows $R(T)$ for segment V_3/V_4 without rf irradiation.

GHz. Figure 2(b) shows similar data for a rf frequency of 50 MHz. For this frequency, the resistance bump appears at temperatures below the midpoint of the transition for low rf power and grows and broadens with increasing rf power until the resistance is raised well above R_N . The effects do not depend on thermal cycling of the sample between 1 and 300 K but are slightly different from sample to sample.

To clarify whether charge imbalance is involved in the effect, we measured over different voltage probes of the same sample in order to check the spatial dependence of the excess voltage. A typical example of normalized $R(T)$ curves obtained over different line segments of the same sample (see Fig. 1) is shown in Fig. 3. At 400 MHz a bump can be induced only in the short segment between the contacts V_1 and V_3 . The other segments of the sample, which are nominally exposed to the same rf current, do not show the pronounced enhancement of R above R_N , but are subjected to the same depression of T_c . T_c is defined as the midpoint of the resistive transition of the segments which do not show the anomaly (see the arrow in Fig. 3). Figures 2(b) and 3 clearly demonstrate that the resistance bump rises below T_c , i.e., in the superconducting state. For the long segment V_3/V_4 , only minor anomalies can be seen at different frequencies, demonstrating that the bump generated in a subsection does not show up if the distance between the probes becomes larger. This is in agreement with the sample length dependence observed by Santhanam *et al.*² and with the idea that the excess voltage is present only when probing the core of the PSC. We have observed similar results for several quasi-1D samples of the same linewidth, while a control measurement on a 2D film only revealed a depression of T_c without any resistance anomalies.

Figure 4(a) shows some voltage current $V(I)$ characteristics of the line segment V_1/V_3 of the mesoscopic sample subjected to the same rf signal of 400 MHz and -50 dB power as in Fig. 3. At temperatures corresponding to the

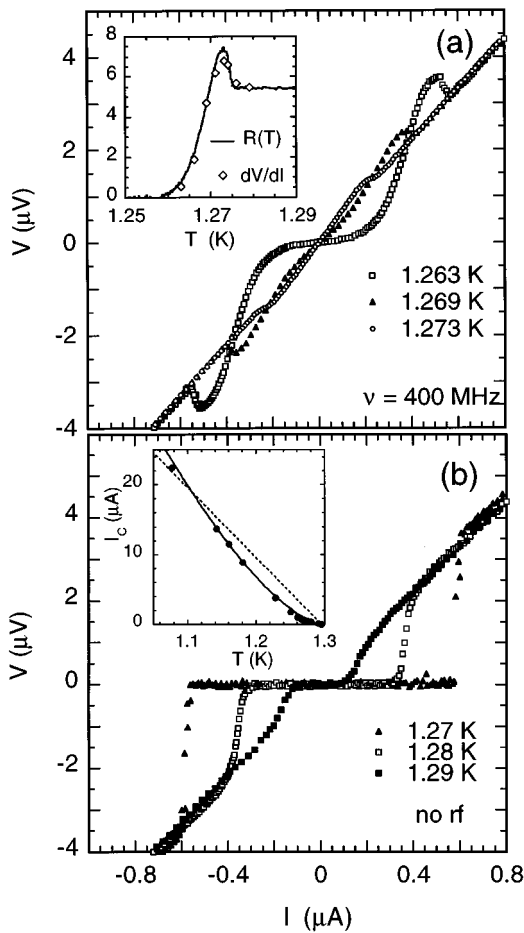


FIG. 4. $V(I)$ characteristics measured over segment V_1/V_3 with (a) a 400 MHz, -50 dB rf signal applied and (b) no rf applied. The inset of (a) compares the resistance obtained from ac resistance measurements and the slope of the $V(I)$ curves for zero current. The inset of (b) shows the critical current versus temperature as obtained from the $V(I)$ curves without rf (dots). The lines are best fits according to $I_c = I_{c0}(T - T_c)^{3/2}$ (solid line) and $I_c \propto (T - T_c)$ (dotted line), respectively. $I_{c0} \cong 340 \mu\text{A}$ corresponds to about 75% of the theoretical depairing current (Ref. 10).

position of the resistance maximum we observe an enhancement of $V(I)$ above the linear Ohmic behavior. The slope of $V(I)$ at zero current matches the height of the observed resistance maximum. With decreasing temperature an anomalous voltage bump develops with locally negative differential resistance. At the same time the zero-current slope goes to zero, corresponding to the transition to the zero-resistance state. The inset in Fig. 4(a) shows good agreement between the $R(T)$ curves obtained from ac resistance measurements at small current ($0.1 \mu\text{A}$) and the slopes of the $V(I)$ characteristics at zero current. In Fig. 4(b) the $V(I)$ curves for the mesoscopic sample, when screened from external rf radiation, are shown. We note that the $V(I)$ curves show no anomalies, indicating the absence of inadvertent noise in our experiment. A 1D line with weak links is expected to give rise to a linear dependence of $I_c(T)$ on $(1 - T/T_c)$.¹⁵ As shown in the inset to Fig. 4(b), we observe power law behavior $I_c(T) = I_{c0}(1 - T/T_c)^{3/2}$ in agreement with the Ginzburg-Landau theory for a 1D wire, clearly supporting

our assumption about the absence of weak links in our sample.

Coming now to the possible microscopic origin of the anomalies which appear in the $R(T)$ and $V(I)$ curves, we refer to the experimental fact that the anomaly clearly develops below the mean-field SC transition temperature. As indicated before, the onset of the resistive behavior in narrow SC lines is governed by the local creation of PSC's. From previous measurements of long microbridges^{11,14} it is known that regions of reduced Δ are the favored locations for the formation of PSC's. These PSC's will create a charge imbalance region, which we believe to be directly responsible for the anomalous resistance bump. The excess voltage in the $V(I)$ characteristic can be understood in terms of the variation of the nonequilibrium chemical potentials on a mesoscopic length scale. Since on short length scales, comparable to the coherence length, the slope $d\mu_{CP}/dx$ may well exceed the slope $d\mu_{QP}/dx$ (see Fig. 3 of Ref. 8), the voltage drop measured with superconducting probes can be considerably larger than the voltage generated in the normal state.

An essential ingredient of our interpretation of the results is obviously related to the local creation of a region of non-equilibrium superconductivity. Kwong *et al.*⁹ and, more recently, Park *et al.*¹⁵ have shown that the generation of a charge imbalance region by introducing N/S interfaces leads to very similar effects. A consistent picture emerges when we assume that the rf radiation induces the local formation of PSC's. This possibility has been demonstrated by Dmitriev and Khristenko.¹⁶ At this point, we do not, however, understand the exact mechanism by which the rf radiation excites the PSC's or the separation of the bump from the transition as in Fig. 2(b).

We note that the presence of a bump in $R(T)$ could also be understood in terms of a simple mixing of the high-frequency signal and the low-frequency or dc measuring current. As the temperature is varied near the transition, the current resulting from the high-frequency signal samples the nonlinear portion of the $V(I)$ curve, resulting in a measured resistance higher than R_N . We have indeed been able to induce a bump in $R(T)$ and related anomalies in the $V(I)$ characteristics with mixing frequencies from 1 kHz to hundreds of MHz. The shape of the superconducting transition is essentially frequency independent below 1 MHz, but changes qualitatively above this frequency.¹⁷ However, the simple mixing effect fails to explain important aspects of our data; for example, the resistance bump appearing below the transition [Fig. 2(b)] or the large excess voltages in the $V(I)$ characteristics near the critical current [Fig. 4(a)].

In summary, we have demonstrated that the remarkable enhancement of the resistance of superconducting mesoscopic structures above the normal-state value can be induced by the presence of a rf electric field. The anomaly in the $R(T)$ curves appears *below* the mean field superconducting transition temperature and is related to anomalies in the $V(I)$ characteristics. We attribute these phenomena to the generation of a local charge imbalance around a phase-slip center.

The work at the K. U. L. has been supported by the Belgian Inter-University Attraction Poles (IUAP) and the Flem-

ish Concerted Action (GOA) programs, while the work at Northwestern University has been supported by the National Science Foundation under Grant Nos. DMR-9357506 and DMR-9313726, the Materials Research Center at Northwest-

ern University under Grant No. NSF-DMR-9120521, and the Alfred P. Sloan Foundation. Travel between Leuven and Evanston was made possible through a NATO Collaborative Research Grant.

-
- ¹For a recent overview see, e.g., *Proceedings of the NATO Advanced Research Workshop on Mesoscopic Superconductivity, Karlsruhe, 1994*, edited by F. W. F. Hekking, G. Schön, and D. Averin [Physica B **203**, 201 (1994)].
- ²P. Santhanam, C. C. Chi, J. Wind, M. J. Brady, and J. J. Bucchignano, Phys. Rev. Lett. **66**, 2254 (1991).
- ³H. Vloeberghs, V. V. Moshchalkov, C. Van Haesendonck, R. Jonckheere, and Y. Bruynseraede, Phys. Rev. Lett. **69**, 1268 (1992).
- ⁴J.-J. Kim, J. Kim, H. J. Shin, H. J. Lee, S. Lee, K. W. Park, and E.-H. Lee, J. Phys. Condens. Matter **6**, 7055 (1994).
- ⁵V. V. Moshchalkov, L. Gielen, G. Neuttiens, C. Van Haesendonck, and Y. Bruynseraede, Phys. Rev. B **49**, 15 412 (1994).
- ⁶M. Tinkham, *Introduction to Superconductivity* (McGraw-Hill, New York, 1975).
- ⁷W. J. Skocpol, M. R. Beasley, and M. Tinkham, J. Low Temp. Phys. **16**, 145 (1974).
- ⁸G. J. Dolan and L. D. Jackel, Phys. Rev. Lett. **39**, 1628 (1977).
- ⁹Y. K. Kwong, K. Lin, P. J. Hakonen, M. S. Isaacson, and J. M. Parpia, Phys. Rev. B **44**, 462 (1991).
- ¹⁰A value of $4 \times 10^{-16} \mu\text{m}^2$ for the ρl product was assumed: J. Romijn, T. M. Klapwijk, M. J. Renne, and J. E. Mooij, Phys. Rev. B **26**, 3648 (1982).
- ¹¹M. Stuiyinga, C. L. G. Ham, T. M. Klapwijk, and J. E. Mooij, J. Low Temp. Phys. **53**, 633 (1983).
- ¹²J. E. Mooij and T. M. Klapwijk, in *Localization, Interaction, and Transport Phenomena*, edited by B. Kramer, G. Bergmann, and Y. Bruynseraede (Springer-Verlag, Berlin, 1985).
- ¹³V. Ambegaokar and A. Baratoff, Phys. Rev. Lett. **10**, 486 (1963).
- ¹⁴W. J. Skocpol and L. D. Jackel, Physica **108B**, 1021 (1981).
- ¹⁵M. Park, M. S. Isaacson, and J. M. Parpia, Phys. Rev. Lett. **75**, 3740 (1995).
- ¹⁶V. M. Dmitriev and E. V. Khristenko, JETP Lett. **29**, 697 (1979).
- ¹⁷B. Burk *et al.* (unpublished).